PACS numbers: 03.65.Xp, **42.25.**–p, **78.67.**–n
DOI: 10.3367/UFNe.0181.201111j.1212

Resonant tunneling of ultrashort electromagnetic pulses in gradient metamaterials: paradoxes and prospects

A B Shvartsburg, N S Erokhin

1. Introduction. Tunneling of a monochromatic wave through a gradient photonic barrier (exactly solvable model)

This report is devoted to new effects of wave-pulse tunneling through inhomogeneous media. The concept of tunneling often refers to quantum effects of particle penetration through potential barriers with the heights exceeding the energy of the particles themselves. It is this problem that was first solved by G A Gamow in 1928 [1] when E Rutherford asked him to explain the paradox of the alpha decay of atomic nuclei, in which the energy of an alpha particle leaving a nucleus proved to be lower than the height of a potential barrier surrounding the nucleus. By using the formal analogy between the classical wave equation and the Schrödinger equation, Gamow managed to show that a partial penetration of de Broglie waves describing an alpha particle through the barrier corresponds to the frustrated total internal reflection effect known in optics. Such a penetration mechanism, which is impossible in classical mechanics, was called 'tunneling'. By connecting this analogy with the uncertainty in the relation between the momentum and coordinate of a quantum particle, Gamow calculated the exponentially small but finite probability of particle tunneling through the barrier. This was probably the first application of quantum mechanics in nuclear physics, and became for many years an etalon for describing the tunneling of quantum objects in electronics and solid state physics.

Tunneling effects attracted new interest with the development of metamaterials and, especially, in connection with advances in nanotechnologies in the manufacturing of so-called gradient media with electromagnetic or mechanical parameters continuously distributed inside a medium according to a specified law managed by the manufacturing technology. Studies were devoted not to traditional quantum problems, but to classical problems of the propagation of electromagnetic waves through gradient finite-thickness dielectric layers. In nanophotonics, such layers are called 'gradient photonic barriers', while in the radiophysics of superhigh-frequency electromagnetic waves, they are called gradient wave barriers. It is these structures that are now attracting attention in the development of a new generation of photonic crystals, guiding wave systems, and miniature radioelectronic devices.

A B Shvartsburg Joint Institute for High Temperatures, Russian Academy of Sciences, Moscow, Russian Federation, and the Space Research Institute, Russian Academy of Sciences, Moscow, Russian Federation
E-mail: alex-s-49@yandex.ru
N S Erokhin Space Research Institute, Russian Academy of Sciences, Moscow, Russian Federation. E-mail: nerokhin@mx.iki.rssi.ru

Uspekhi Fizicheskikh Nauk **181** (11) 1212–1217 (2011)
DOI: 10.3367/UFNr.0181.201111j.1212
Translated by M N Sapozhnikov; edited by A Radzig

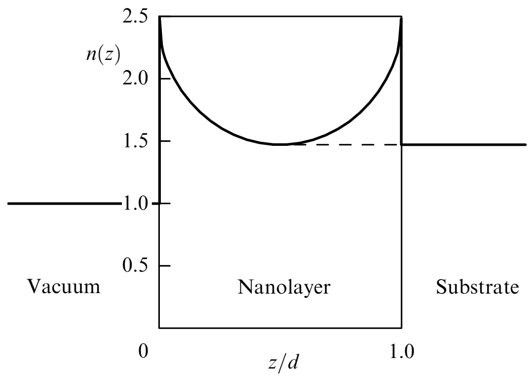

Figure 1. Normalized permittivity profile (1) inside a gradient photonic barrier providing the tunneling of electromagnetic waves through a barrier with width d; z/d is the dimensionless coordinate across the barrier.

As shown in review [2], the physical foundations of tunneling electromagnetic waves through gradient media are determined by geometrical or nonlocal dispersion. This mechanism is not related to the material dispersion of the barrier material and depends on the gradient and curvature of the spatial profile of the refractive index $n(z)$. Artificial dispersion effects are considered in this paper for transparent barriers obtained by the deposition of a dielectric onto a homogeneous nonabsorbing substrate with the refractive index n. The exact analytical solutions to Maxwell's equations for a number of such gradient photonic barriers demonstrate the peculiarity of wave tunneling processes in gradient nanooptics, which consists, in particular, of the following [3]:

(1) The reflection and transmission spectra of gradient media are determined not only by the jump of the refractive index $n(z)$ on the medium boundary, but also by the discontinuities of the gradient and curvature of the refractive index profile $n(z)$. The expressions for reflection and transmission spectra were obtained for a number of $n(z)$ profiles, the classical Fresnel formulae being merely a particular case of these expressions. Thus, the normalized $n(z)$ profile (Fig. 1) containing two arbitrary spatial scales L_1 and L_2, namely

$$n(z) = n_0 U(z)\,, \qquad U(z) = \left(1 + \frac{z}{L_1} - \frac{z^2}{L_2^2}\right)^{-1}, \tag{1}$$

is characterized by the cutoff frequency Ω [3] depending on the barrier thickness d, the refractive index n_0 of the barrier material, and geometrical parameters of profile (1):

$$\Omega = \frac{2cy\sqrt{1+y^2}}{n_0 d}\,, \qquad y = \frac{L_2}{2L_1}\,. \tag{2}$$

The transmittance of a gradient wave barrier (1) with cutoff frequency (2) is determined by the waveguide type dispersion: waves with frequencies $\omega > \Omega$ propagate through the barrier in the traveling-wave regime, while waves with frequencies $\omega < \Omega$ propagate in the tunneling regime. The tunneling spectra of barrier (1) can be conveniently considered using the dimensionless frequency $u = \Omega/\omega$. In this case, the regime of $\omega > \Omega$ $(\omega < \Omega)$ corresponds to the condition $u < 1$ $(u > 1)$. The complex transmission coefficient $T = |T| \exp(\mathrm{i}\phi_t)$ of barrier (1) in the traveling-wave regime is described by the expressions [3]

$$|T|^2 = \frac{4nn_e^2(1+t^2)}{|\Gamma|^2}, \tag{3}$$

$$|\Gamma|^2 = \left[t\left(n - \frac{\gamma^2}{4} + n_e^2\right) + \gamma n_e\right]^2 + (n+1)^2\left(n_e - \frac{\gamma t}{2}\right)^2, \tag{4}$$

$$\cos\phi_t = \frac{(n+1)(n_e - \gamma t/2)}{|\Gamma|}, \quad \sin\phi_t = \frac{t(n - \gamma^2/4 + n_e^2) + \gamma n_e}{|\Gamma|}, \tag{5}$$

$$t = \tan\left(l\sqrt{\frac{1}{u^2} - 1}\right), \qquad n_e^2 = n_0^2(1 - u^2), \tag{6}$$

$$\gamma = \frac{2n_0 uy}{\sqrt{1+y^2}}, \qquad l = \ln\frac{y_+}{y_-}, \qquad y_\pm = \sqrt{1+y^2} \pm y. \tag{7}$$

The complex transmission coefficient $T = |T|\exp(\mathrm{i}\phi_t)$ of the barrier in the tunneling regime is described by other expressions

$$|T|^2 = \frac{4nn_e^2(1-t^2)}{|\aleph|^2}, \tag{8}$$

$$|\aleph|^2 = \left[t\left(n - \frac{\gamma^2}{4} - n_e^2\right) + \gamma n_e\right]^2 + (n+1)^2\left(n_e - \frac{\gamma t}{2}\right)^2, \tag{9}$$

$$\cos\phi_t = -\frac{(n+1)(n_e - \gamma t/2)}{|\aleph|}, \quad \sin\phi_t = -\frac{t(n - \gamma^2/4 - n_e^2) + \gamma n_e}{|\aleph|}, \tag{10}$$

$$n_e^2 = n_0^2(u^2 - 1), \qquad t = \tanh\left(l\sqrt{1 - \frac{1}{u^2}}\right). \tag{11}$$

Parameters γ and l entering formulas (8)–(11) are defined in Eqn (7).

(2) Analysis of expressions (3)–(11) for the complex transmission coefficient $T = |T|\exp(\mathrm{i}\phi_t)$ shows that, on passing from the traveling-wave regime to the tunneling regime ($u = 1$), the modulus of the coefficient, $|T|$, changes continuously (Fig. 2a), while the phase ϕ_t experiences a jump by π (Fig. 2b).

(3) The permittivity, unlike that in conventional electromagnetic-wave tunneling effects in media with free carriers, preserves the positive real value at all points inside a nanofilm ($0 < z < d$), in particular, on the descending branch of the $\varepsilon(z)$ profile ($0 \leqslant z \leqslant d/2$), where the condition $\operatorname{grad}\varepsilon < 0$ is fulfilled for $\varepsilon > 0$. The interference of the forward and backward waves in the gradient barrier can lead not to the known effects of strong reflection of the incident wave and exponential decay of the tunneling field in a homogeneous rectangular barrier, but to an almost reflectionless (resonance) tunneling regime in some spectral interval. The transmission coefficient squared $|T|^2$ in such a state can reach high values of $|T|^2 = 0.9{-}0.95$, and even $|T|^2 = 1$.

2. Dynamics of an ultrashort pulse during resonance tunneling

The properties of monochromatic fields pointed out in Refs [2, 3] are used here to analyze the tunneling of ultrashort broadband one- or few-cycle femtosecond pulses and video pulses through a gradient photonic barrier. The tunneling of such pulses is considered below without any new physical hypothesis and mathematical approximations based on Maxwell's equations for the exactly solvable model of this barrier.

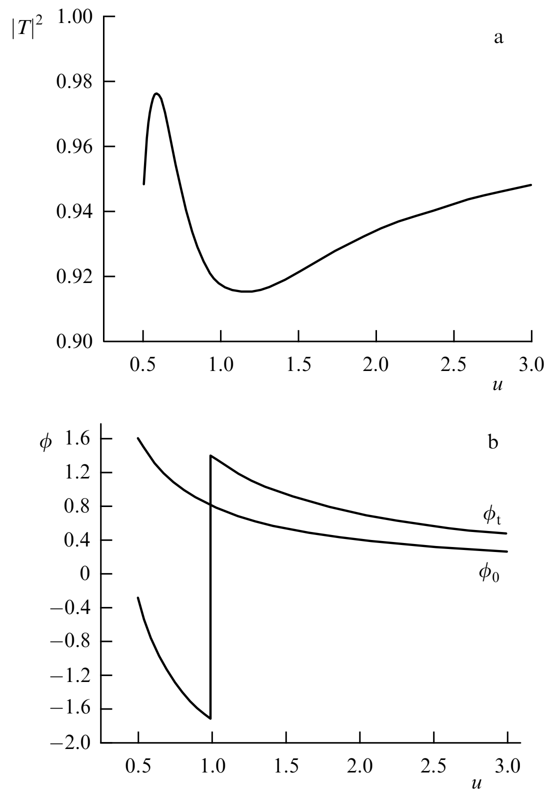

Figure 2. Tunneling spectra for the gradient barrier depicted in Fig. 1, with parameters $n_0 = 2.3$, $n_{min} = 1.47$, and $d = 100$ nm. (a) Energy transmission coefficient $|T|^2$. (b) Phase shift ϕ_t of the transmitted wave; ϕ_0 is the wave phase incursion in air, and $u = \Omega/\omega$ is the normalized frequency.

Consider a barrier formed by a transparent dielectric nanolayer with width d and continuous profile (1) plotted in Fig. 1 (curve *1*). The nanolayer is deposited onto a thick homogeneous substrate with the refractive index n. The refractive index achieves maximum values of $n = n_0$ on the layer boundaries $z = 0$ and $z = d$, and a minimum value of $n = n_{min}$ at $z = 0.5d$. The cutoff frequency Ω of such a gradient barrier is determined by expression (4). The amplitude–phase transmission spectra in the vicinity of the normalized cutoff frequency $u = \Omega/\omega = 1$, plotted by expressions (3)–(11) for the complex transmission coefficient $T = |T|\exp(\mathrm{i}\phi_t)$ of the barrier, are displayed in Fig. 2.

One can see from Fig. 2 that the energy transmission coefficient $|T|^2$ for $u = 1$ is continuous, whereas the phase spectrum of the transmitted wave for $u = 1$ exhibits a jump by π [4]: the values of $\phi_t(\omega)$ in the tunneling regime ($\omega \leqslant \Omega$, $u \geqslant 1$) are positive, and they are negative in the traveling-wave regime ($\omega \geqslant \Omega$, $u \leqslant 1$). The phase shift ϕ_t in the tunneling regime can exceed in some frequency interval the phase shift ϕ_0 of a wave with the same frequency ω propagating through the same distance d in free space ($\phi_0 = \omega d/c$). These superluminal ($\phi_t > \phi_0$) and subluminal ($\phi_t < \phi_0$) phase effects are exemplified in Fig. 2b.

Consider the tunneling of a femtosecond pulse with duration t_0, carrier frequency ω_0, amplitude E_0, and envelope

$$E(t) = E_0 \sin\frac{\pi t}{t_0}\cos(\omega_0 t), \tag{12}$$

incident normally on a gradient barrier with the transmission spectra displayed in Fig. 2. The spectrum of pulse (12) contains harmonics belonging both to the traveling-wave and tunneling regions. The phase shifts ϕ_t in these regions have opposite signs, and the frequency dispersion of phase spectra is considerable in both regions (Fig. 2b). The contributions of harmonics with $\phi_t < 0$ and $\phi_t > 0$ to the envelope of the tunneling pulse prove to be dependent on the detuning of the carrier frequency ω_0 from the cutoff frequency Ω. The pulse envelope after tunneling through the gradient barrier is constructed by using the inverse Fourier transform of the product $F(\omega)\,T(\omega)$, where $F(\omega)$ is the Fourier transform of an initial pulse (12), and $T(\omega)$ is the complex transmission coefficient. To take into account contributions from both subluminal and superluminal phase shifts to the formation of the tunneling envelope $E_1(t)$, the inverse Fourier transform is performed in the ω-frequency range from 0 to ∞.

The tunneling pulse dynamics can be conveniently considered in a coordinate system moving together with the leading edge of the pulse in free space at the velocity c. The points of the envelope located behind (ahead) of this leading edge correspond to positive (negative) times, the pulse onset corresponding to the instant $t = 0$. Figure 3 plotted in this coordinate system shows the superluminal displacements of the deformed envelope caused by tunneling frequencies ($u > 1$) in the region $t < 0$ [4]; propagating frequencies ($u < 1$) determine deformation in the subluminal region $t > 0$. The inequality between phase shifts of different harmonics leads to the oscillating broadening of the transmitted pulse and the superluminal shift of its leading edge accompanied by some loss in the pulse energy [$|T|^2 = 0.91$–0.92 (Fig. 2a)]. The normalized envelopes $E_1(t)/E_0$ of transmitted pulses are depicted in Fig. 3. A comparison of these envelopes shows that the distortion of tunneling pulses critically depends on the carrier-frequency detuning $\Delta = (\omega_0 - \Omega)/\Omega$ with respect to the cutoff frequency Ω.

Figure 3a, corresponding to the negative detuning $\Delta = -8.16 \times 10^{-2}$, gives evidence that precursors formed at the leading edge of the tunneling pulse are located in the region $t < 0$, therefore leaving behind the leading edge of the freely propagating pulse ($t = 0$); the amplitude of these precursors, equal to 0.2 at the point $t = 0$, decreases sidewise of the pulse propagation. The modulation of the trailing edge in the region $t > 0$ is provided by propagating frequencies ($u < 1$). In the case of the zero detuning ($\omega_0 = \Omega$ and $\Delta = 0$), the pulse is completely split, producing two peaks with the amplitude 0.7; the precursor amplitude on the pulse leading edge at the point $t = 0$ increases to 0.48. Finally, as the carrier frequency shifts to the traveling region ($\Delta = 4.08 \times 10^{-2} > 0$), the modulation of the fronts of the tunneling pulse and splitting of the maximum become less pronounced (Fig. 3d).

Notice that these deformations appear when pulse (12) propagates through a thin gradient barrier with width $d = 100$ nm much smaller than the wavelength λ (800 nm) corresponding to the carrier frequency ω_0. This effect is typical precisely for a gradient barrier: one can see from Fig. 4 that when pulse (12) with the same carrier frequency ω_0 propagates through a homogeneous barrier, which does not have the cutoff frequency ($\Omega = 0$) and has all the other parameters $(n_0, n_{\min}, n, d)$ coinciding with those for the above-discussed gradient barrier, the tunneling regime and pulse splitting do not appear.

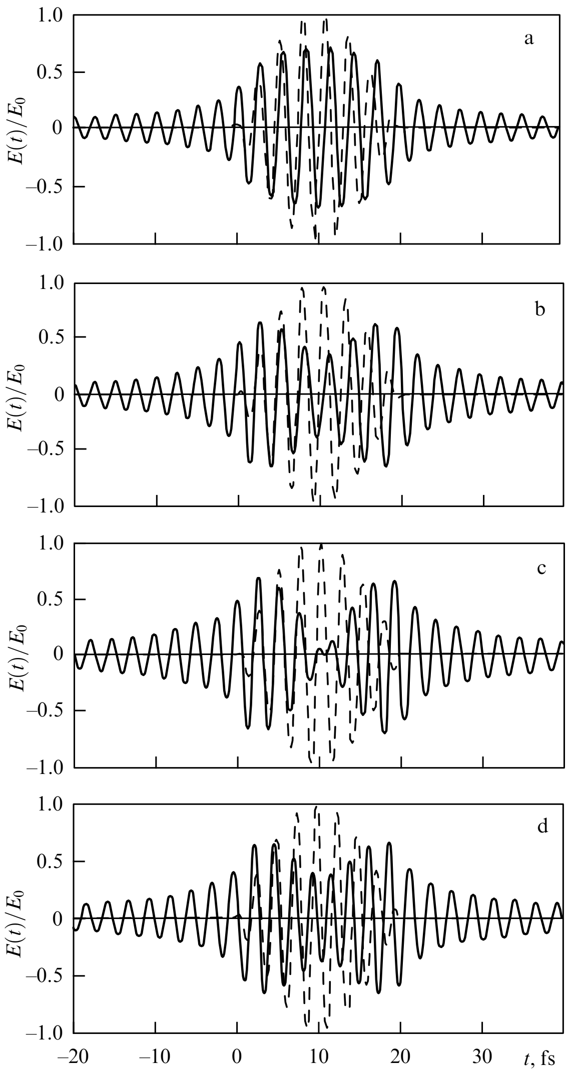

Figure 3. Normalized time envelopes $E(t)/E_0$ of a femtosecond pulse (12) ($t_0 = 20$ fs) propagating in free space (dashed curves), and a pulse tunneling through a gradient barrier (solid curves), $\Omega = 2.45 \times 10^{15}$ rad s^{-1}; carrier frequencies and detunings in Figs 3a–d are $\omega_0 = 2.25 \times 10^{15}$, 2.35×10^{15}, 2.45×10^{15}, and 2.55×10^{15} rad s^{-1}, and $\Delta = -8.16 \times 10^{-2}$, -4.08×10^{-2}, 0, and 4.08×10^{-2}, respectively. Superluminal precursors are formed in the region of $t < 0$.

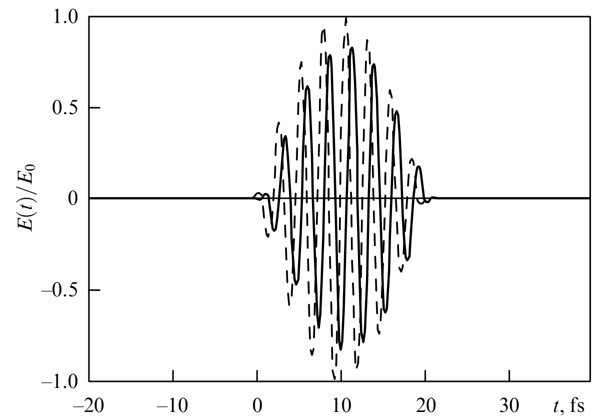

Figure 4. Transmission of pulse (12) with $\omega_0 = 2.45 \times 10^{15}$ rad s^{-1} in the traveling-wave regime through a homogeneous wave barrier ($\Omega = 0$) with parameters n_0, $n_{\min}$, n, and d indicated in the caption to Fig. 2. Unlike the tunneling regime (Fig. 3), no pulse precursors are formed.

It should be noted that during tunneling the 'center of gravity' t_c of the pulse $f(t)$ shifts with respect to the center t_{c0} of a pulse propagating in a vacuum at the speed of light, $\Delta_t = t_{c0} - t_c$, where

$$t_c = \frac{\int_{-\infty}^{\infty} t f(t)\,\mathrm{d}t}{\int_{-\infty}^{\infty} f(t)\,\mathrm{d}t}\,. \tag{13}$$

Calculations using expression (13) reveal that, during tunneling of pulse (12) ($t_0 = 20$ fs), the pulse shift $\Delta_t \approx 0.15-0.2$ fs, i.e., the center of gravity of the pulse after tunneling *lags* behind the center of gravity of a freely propagating pulse ($\Delta_t > 0$).

3. Formation of superluminal precursors during tunneling of a short pulse

At first glance, the modulation of the envelope at the pulse edges resembles the classical Sommerfeld–Brillouin effect — the formation of precursors during the propagation of a pulse in a transparent dispersive medium outside the tunneling region. It is well known that the formation path of these precursors should be long enough ($Z \gg ct_0$), their amplitude should be small compared to the peak amplitude of the pulse, and their velocity does not exceed the speed of light c in a vacuum [5]. However, the results of formation of superluminal precursors [4] during pulse tunneling through a gradient barrier (see Fig. 3) strongly differ from those in the classical picture.

(1) Because of the phase jump producing the fast shift of tunneling harmonics, the considerable deformation of the pulse is developed at distances smaller than the wavelength.

(2) The amplitudes of precursors are not small and can be comparable to the initial pulse peak.

(3) The partial or complete pulse splitting resulting in the formation of precursors is determined by the frequency detuning Δ.

Speaking of the formation of superluminal precursors of the pulse transmitted through a gradient barrier in the tunneling regime, we should point out differences between the basic parameters of the transmitted and initial pulses:

(a) the energy of the transmitted pulse is lower than that of the initial pulse, while its duration is longer compared to the initial pulse. Moreover, the envelope of the transmitted pulse has nothing in common with the initial envelope;

(b) the rate v_g of energy transfer by the tunneling wave inside the barrier, defined as $v_g = P/W$, where P is the Umov–Poynting vector, and W is the energy density, is less than the speed of light c in a vacuum (Fig. 5);

(c) the center of gravity of the transmitted pulse lags behind the center of gravity of the same freely propagating pulse.

The precursor formation rate depends on the number m of field oscillations inside the tunneling pulse with the carrier frequency ω_0 and duration t_0 ($m \approx \omega_0 t_0/(2\pi)$) and the amplitude build-up rate from a periphery to maximum, this rate being related to the parameter m. Under conditions specified in the caption to Fig. 3 ($m = 7-8$), precursors and the splitting of the maximum are well pronounced, while in the case of $t_0 = 100$ fs at the same carrier frequency, m is much greater ($m = 37-38$), the amplitude build-up rate is slower, and a weak modulation appears only in the envelope wings (Fig. 6), while the central peak is not split. To exclude the possible influence of artificial 'end points' of the envelope appearing in model (12), paper [4] reported on the tunneling

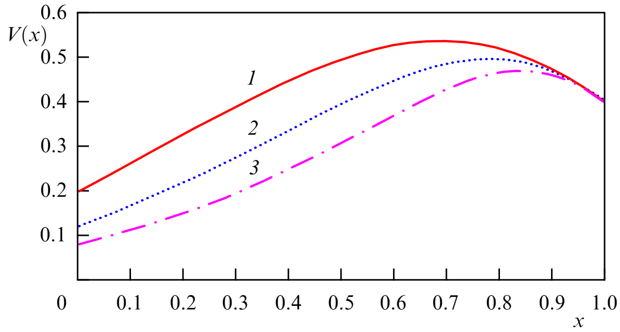

Figure 5. Dispersion of the normalized group velocity $V(x) = v_g/c$ inside the gradient photonic barrier shown in Fig. 1; $x = z/d$ is the dimensionless coordinate. Curves *1*, *2*, and *3* correspond to normalized frequencies $u = 1.0$, 1.5, and 2.0.

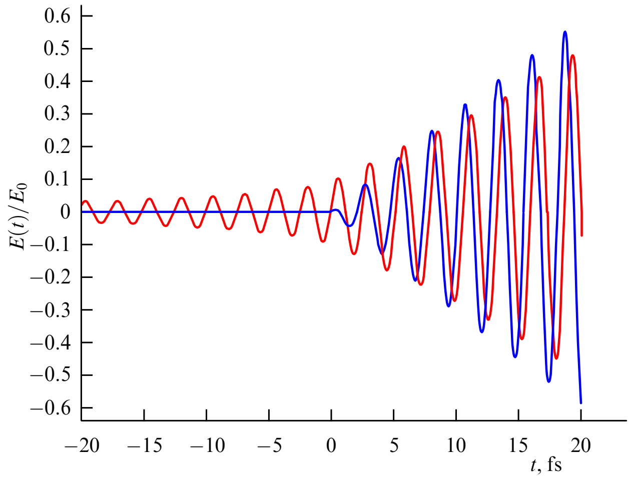

Figure 6. Weak modulation of the envelope ($E/E_0 \leqslant 0.05$) at the periphery of the 'long' pulse (12) ($t_0 = 100$ fs) tunneling through a barrier under conditions of Fig. 3; $\omega_0 = 2.562 \times 10^{15}$ rad s^{-1}.

dynamics of a 'smooth' Gaussian pulse, in which a slow decrease of the envelope in the wings is not related to these points:

$$E(t) = E_0 \exp\left(-\frac{t^2}{t_1^2}\right) \cos(\omega_0 t)\,. \tag{14}$$

The characteristic time t_1 in formula (14) is selected so that t_0, determining the duration of pulse (12), corresponds to the half-width of the Gaussian pulse (14), i.e., $t_1 = 1.2 t_0$.

A comparison of the tunneling of pulses (12) and (14) through the same barrier at the same carrier frequencies ω_0 shows that the envelope experiences splitting in the case of a Gaussian pulse as well, and a superluminal precursor is formed at its leading edge.

Similar effects are also observed during tunneling of ultrashort broadband video pulses containing one or several anharmonic field oscillations and a long decaying 'tail' [6]. An example of such a transformation of a video pulse with the envelope constructed from the Laguerre functions, namely

$$\frac{E(t)}{E_0} = \frac{1}{2}\,x(x-4)\exp\left(-\frac{x}{2}\right), \qquad x = \frac{t}{t_0}\,, \tag{15}$$

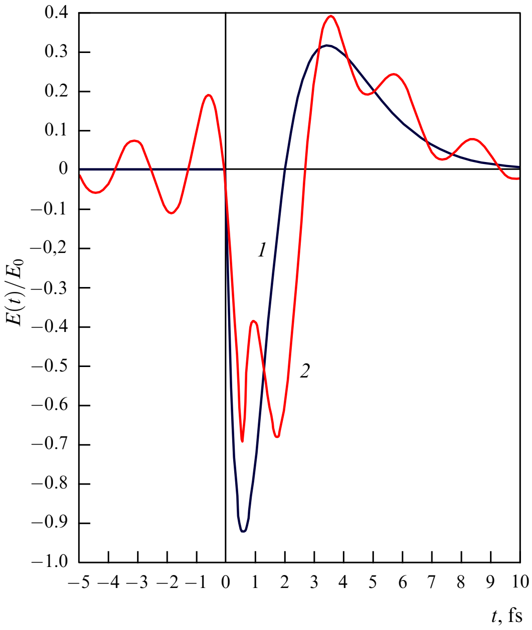

Figure 7. Fast modulation of the video pulse (15) and formation of superluminal precursors during tunneling through a gradient barrier; *1* and *2* are the time envelops of the incident and transmitted pulses ($t_0 = 0.5$ fs). Superluminal precursors are formed at the leading edge of the video pulse ($t < 0$).

where t_0 is the characteristic time scale, is presented in Fig. 7.

Speaking of superluminal precursors, note that the question about the tunneling rate became a sticking point in the tunneling theory beginning already in Gamow's time. Thus, the attempt by Condon and Morse [7] to calculate, using this theory, the velocity or the flight time of a particle in the region where the particle energy E is smaller than the potential barrier height U_0 revealed the principal problem: how to determine these quantities in the 'classically forbidden' region, where the particle momentum should be treated as an imaginary quantity? A year later, MacColl [8] concluded that "a wave packet moving inside a barrier exhibits no delay". Later on, the concept of the complex time attracted attention in the analysis of the fundamental-mode tunneling in a metal waveguide through a region with a lower cutoff frequency [9]. According to this concept, the tunneling time τ in the problem under study was expressed in terms of the complex transmission function $T = |T| \exp(\mathrm{i}\phi_t)$:

$$\tau = \sqrt{\left(\frac{\partial \phi_t}{\partial \omega}\right)^2 + \left(\frac{\partial \ln |T|}{\partial \omega}\right)^2}\,. \qquad (16)$$

On the threshold of the centenary of the special theory of relativity (2005), new formulations of the causality principle, including tunneling effects, also appeared. For example, the output energy flux from a stationary medium at any instant cannot exceed the flux that would be present in the absence of the medium [10]. However, this formulation leads to contradictory judgements [11, 12], and the question of defining the tunneling time remains open.

4. Conclusions

Speaking about the controllable dispersion of waves in gradient media, it is worthwhile noting a number of its features which can be used for the development of gradient structures for optoelectronics:

(1) To produce a gradient wave barrier in the specified spectral range, an artificial material can be utilized with the absorption spectrum lying far from the strong dispersion region, unlike the absorption spectra of natural materials, which are usually located close to the strong dispersion region.

(2) The appearance of the controllable cutoff frequency in gradient dielectrics opens up the possibility of using such dielectrics instead of metal films in photonic crystal elements and other devices in plasmonics.

(3) The universal character of the above-mentioned effects based on the exact analytical solutions of Maxwell's equations for inhomogeneous media allows one to extend the obtained results to other spectral regions, for example, the gigahertz range. This analogy permits the parallel development and simulation of subwave optical, gigahertz, and quantum structures with such sets of parameters which are not encountered in natural materials.

Notice also that the formation mechanism of superluminal pulse precursors during tunneling through gradient photonic nanobarriers has been described here by exact analytical solutions of Maxwell's equations and does not require new physical hypothesis. Moreover, the use of weakly decaying tunneling modes eliminates the problem of recording exponentially decaying modes in conventional tunneling experiments. In this situation, tunneling experiments in optical and microwave regions of electromagnetic waves become decisive [13]; as pointed out above, the transmitted pulse, in which the envelope experiences a superluminal pulse shift in some part due to tunneling, has nothing in common with the incident pulse (the energy of the transmitted pulse is lower and its duration is longer than those of the incident pulse, and the temporal and spectral envelopes of these pulses are different), so that the Einstein treatment of the speed of light in vacuum as the limiting speed of motion of any object in a free space ("the speed of light in vacuum cannot depend on the source velocity" [14]) is not violated in the tunneling picture under study. However, the study of the superluminal pulse advance of some part of the pulse compared to the same pulse propagating in vacuum can be of not only academic but also practical interest, opening new possibilities for applications.

Acknowledgments

The authors thank T Arecci, L M Zelenyi, M A Zuev, V Kuzmiak, A A Maradudin, G Petite, O V Rudenko, and V E Fortov for useful discussions of the results of this paper.

References

1. Gamow G *Z. Phys.* **51** 204 (1928)
2. Shvartsburg A B *Usp. Fiz. Nauk* **177** 43 (2007) [*Phys. Usp.* **50** 37 (2007)]
3. Shvartsburg A B, Kuzmiak V, Petite G *Phys. Rep.* **452** 33 (2007)
4. Shvartsburg A B, Petite G, Zuev M *J. Opt. Soc. Am. B* **28** 2271 (2011)
5. Ginzburg V L *Rasprostranenie Elektromagnitnykh Voln v Plazme* (The Propagation of Electromagnetic Waves in Plasmas) (Moscow: Nauka, 1967) [Translated into English (Oxford: Pergamon Press, 1970)]
6. Shvartsburg A B *Impulse Time-Domain Electromagnetics of Continuous Media* (Boston: Birkhäuser, 1999)
7. Condon E U, Morse P M *Rev. Mod. Phys.* **3** 43 (1931)
8. MacColl L A *Phys. Rev.* **40** 621 (1932)

9. Buttiker M, Landauer R *J. Phys. C Solid State Phys.* **21** 6207 (1988)
10. Steinberg A M, Kwiat P G, Chiao R Y *Phys. Rev. Lett.* **71** 708 (1993)
11. Nimtz G, Enders A, Spieker H *J. Physique I* **4** 565 (1994)
12. Milonni P W *J. Phys. B At. Mol. Opt. Phys.* **35** R31 (2002)
13. Shvartsburg A B et al. *Phys. Rev. E* **78** 016601 (2008)
14. Einstein A "On the electrodynamics of moving bodies", in *The Collected Papers of Albert Einstein* Vol. 2 *The Swiss Years: Writings, 1900 – 1909* (Eds J Stachel et al.) (Princeton, N.J.: Princeton Univ. Press, 1989)

PACS numbers: **43.20.+g**, **43.30.+m**, **43.60.–c**
DOI: 10.3367/UFNe.0181.201111k.1217

Focusing of low-frequency sound fields on the ocean shelf

V G Petnikov, A A Stromkov

1. Introduction

The utility of focused low-frequency (100–500 Hz) sound for solving a variety of applied tasks of sea-shelf acoustics is presently a subject of ongoing research. The case in point concerns focusing of sound waves at distances of several dozen kilometers from focusing systems in a sea with a typical depth of 100 m.

From a physical viewpoint, the question to be answered is how to focus sound waves in a planar waveguide, the parameters of which (depth, refractive index, and acoustic characteristics of the lower boundary set by the oceanic bottom) are some complex functions of space coordinates. It is essential that part of these parameters, primarily the refractive index, exhibit random fluctuations in space and time. Furthermore, the distance to the focal point far exceeds the size of the focusing system.

Under these circumstances, perhaps the only way to focus sound waves consists in adopting methods based on the generation by the focusing system of a wave field that is conjugate to the medium. Such methods include the wave front reversal (WFR) (or phase conjugation) of sound waves and a similar approach based on time wave reversal [1–3], dubbed the time-reversal mirror (TRM). It should be kept in mind that both methods rely on detecting sound waves emitted by a probe source (PS) placed at the supposed focal point and subsequent generation of the reversed wave field by the focusing system backwards into the waveguide. Sound propagation in the opposite direction through just the same inhomogeneities as encountered on the direct way leads to the compensation of phase and time distortions of the acoustic signals and, as a result, to focusing on the PS site.

This paper describes methods and research results related to unusual properties of focused sound in shallow water. It discusses characteristics of physical setups designed for focusing sound waves in conditions that are very experimentally demanding. It also considers possible areas where the focused sound can be utilized.

V G Petnikov A M Prokhorov General Physics Institute, Russian Academy of Sciences, Moscow, Russian Federation
E-mail: petniko@kapella.gpi.ru
Stromkov A A Institute of Applied Physics, RAS, Nizhny Novgorod, Russian Federation

Uspekhi Fizicheskikh Nauk **181** (11) 1217 – 1222 (2011)
DOI: 10.3367/UFNr.0181.201111k.1217
Translated by S D Danilov; edited by A Radzig

2. Methods of the investigation of focused sound in shallow water

Studies of specific features of sound focusing in ocean shelf have been carried out both through numerical simulations and on-site experiments (see, for example, Refs [4–6]). Generally, the TRM-based focusing effect in some vicinity of point $\mathbf{r}_0$ was computed for the spatial distribution of the quantity $B(\mathbf{r})$:

$$B(\mathbf{r}) = \max_t \left(B_c(\mathbf{r}, t)\right) = \max_t \left[\frac{1}{T}\left|\int_{-\infty}^{\infty} P(\omega, \mathbf{r})\, s(\omega) \exp(-\mathrm{i}\omega t)\, \mathrm{d}\omega\right|\right]. \tag{1}$$

The function $B_c(\mathbf{r}, t)$ represents here the envelope of the cross-correlation function of the transmitted and received retransmitted signals, which can, strictly speaking, be defined for broadband signals of finite duration; the maximum is sought with respect to time t; $\mathbf{r}_0$ is the radius vector of the focal point (the point where the PS is located); $s(\omega)$ is the spectrum of the transmitted signal; T is its duration, and $P(\omega, \mathbf{r})$ is the spectrum of the retransmitted signal at some point $\mathbf{r}$:

$$P(\omega, \mathbf{r}) = \sum_j^J Z_1(\omega, \mathbf{r}_j, \mathbf{r})\, Z^*(\omega, \mathbf{r}_0, \mathbf{r}_j)\, s^*(\omega), \tag{2}$$

with the asterisk $*$ denoting a complex conjugation. Here, $Z(\omega, \mathbf{r}_0, \mathbf{r}_j)$ and $Z_1(\omega, \mathbf{r}_j, \mathbf{r})$ are the waveguide transfer functions between points $\mathbf{r}_0$ and $\mathbf{r}_j$, and $\mathbf{r}_j$ and $\mathbf{r}$, respectively, and, finally, $\mathbf{r}_j$ is the radius vector of transceivers (receiving and emitting elements) of the focusing system. It is assumed that the role of such a system is played by a discrete vertical antenna composed of J transceivers (just such antennae are used in conventional hydroacoustic on-site experiments to transmit and receive low-frequency hydroacoustic signals).

When applied to the focusing of a quasiharmonic sound field of frequency $\omega = \omega_0$ and arbitrarily long duration, formula (1) converts to the well-known expression for the field amplitude at the observation point:

$$P_a(\omega_0, \mathbf{r}) = \left|\sum_j^J Z_1(\omega_0, \mathbf{r}_j, \mathbf{r})\, Z^*(\omega_0, \mathbf{r}_0, \mathbf{r}_j)\right| s_0. \tag{3}$$

Formula (3) describes focusing with the help of WFR for a harmonic PS with the amplitude s_0. As shown by Zverev [3], the two methods of focusing (based on WFR and TRM) possess principal distinctions, which has just been corroborated by numerical modeling.

In numerical simulations, the transfer functions were taken as sums of interacting waveguide modes. In particular, the following expression served to compute the $Z(\omega, \mathbf{r}_0, \mathbf{r}_j)$ function:

$$Z(\omega, \mathbf{r}_0, \mathbf{r}_j) = \sum_m^{M(\omega)} C_m(\omega, \mathbf{r}_0, \mathbf{r}_j)\, \frac{\psi_m(\omega, z_j)}{\sqrt{q_m(\omega) r_0}} \exp\left(\mathrm{i} q_m(\omega) r_0\right), \tag{4}$$

where $\psi_m(\omega, z)$ and $\xi_m(\omega)$ are the eigenfunctions (waveguide modes) and eigenvalues of the related Sturm–Liouville problem $[\xi_m(\omega) = q_m(\omega) + \mathrm{i}\gamma_m(\omega)/2]$, respectively, and $M(\omega)$ is the number of propagating modes. The expression for $Z_1(\omega, \mathbf{r}_j, \mathbf{r})$ is written out in a similar way [6].